End-pumped Nd:YAG zigzag slab laser with weak pump absorption

Xing Fu (付 星), Qiang Liu (柳 强)*, Xingpeng Yan (闫兴鹏), Jinyu Cui (崔进宇), and Mali Gong (巩马理)

Center for Photonics and Electronics, State Key Laboratory of Tribology, Department of Precision Instruments, Tsinghua University, Beijing 100084, China

**E-mail: qiangliu@mail.tsinghua.edu.cn*

Received September 23, 2008

A diode-pumped Nd:YAG oscillator laser with an end-pumped zigzag slab architecture and weak pump absorption is developed. An output power of 253 W with a slope efficiency of 50.2% and an optical-optical conversion efficiency of 39.6% is achieved from the resonator, which emits the maximum power of 290 W with 840-W pump power. An optimum laser diode (LD) array coolant temperature is chosen in an attempt to realize the weak but uniform pump absorption. Furthermore, we have confirmed that the performance of zigzag slab resonator depends sensitively on the incident angle of the beam at the slab end face.

OCIS codes: 140.3480, 140.3580, 140.4780.

doi: 10.3788/COL20090706.0492.

Diode-pumped slab lasers have recently attracted much more interest for their compact structure, high stability, power scalability, and good beam quality. Various configurations have been proposed for slab lasers, e.g., zigzag slab lasers[1−3], slab oscillators[4−10], multi-stage slab amplifiers[11−13], and multi-pass slab amplifiers[14,15]. Goodno *et al.* presented a novel end-pumped zigzag slab laser architecture, using which they demonstrated a single-head Yb:YAG power oscillator emitting 415 W of multi-mode power and 252 W with linear polarization and M^2 factor below 1.5[3]. Slab laser has been proven to be an effective architecture to reduce thermally induced stress and aberration. However, control on thermal effects still plays a very important role in the end-pumped slab laser. Especially, for thermally bonded composite crystal in end-pumped slab configuration, extremely large thermal gradient arises from the heat deposition within a small volume near the bonding region, which results in severe thermal lensing and aberration and thus low output power. In this letter, an end-pumped Nd:YAG zigzag slab laser with weak pump absorption is demonstrated, in an attempt to increase the uniformity of pump distribution and enhance the output power.

The experimental setup of the end-pumped zigzag slab laser architecture is depicted in Fig. 1. The dimension of the composite slab is 8×2×78 (mm) (width×thickness×length). The central 50-mm section of the slab is 0.5 at.-% doped Nd:YAG, with 14-mm-long diffusion-bonded undoped YAG end caps. The end caps reduce thermal distortions in the slab tips by confining heat generation to portions of the slab that can be effectively cooled, and then prevent the thermal fracture under high power intensity pumping. Moreover, the slab is beveled at edge faces in order to suppress the parasitic oscillation. The slab is conduction cooled on the top and bottom faces. For better cooling of the slab, water-cooled copper micro-channel heat sinks are designed with fin and channel widths of 0.2 mm, fin height of 1 mm, and base thickness of 0.5 mm, and are thermally contacted to the slab total-internal-reflection (TIR) faces using a thin indium film thermal layer.

A SiO_2 coating deposited on TIR surfaces ensures TIR zigzag reflections for the laser beam with minimum loss by allowing the evanescent wave to be attenuated. The slab ends are cut at 45° and anti-reflection (AR) coated at 1064 nm for incident angle from 15° to 25°. An AR coating at 808 nm is also deposited on each of the end-coupling areas on the top and bottom faces of the slab. The slab is pumped from each end by an array of 10 laser diode (LD) bars (Dilas diodes) with an emitting area of 16.2×10 (mm). Each array, with the fast axis collimated by microlenses, emits a maximum output power of 1000 W at a wavelength around 808 nm at the coolant temperature of 25°. The output power from LD array, shaped and focused by two generatrix-orthogonal cylinder lenses, undergoes TIR at the slanted undoped end face of the slab, and is absorbed along the length of the doped region. The resonator consists of a total-reflection concave mirror (HR) with a 1000-mm radius of curvature and a concave output mirror (OC) of 40% transmission with a 1000-mm radius of curvature. Both mirrors are positioned at the distance of $d_1 = d_2 = 25$ mm from the slab end.

Before the implementation of experiment, we have to decide the incident angle θ of laser beam at the slab end, that is, the angle between the normal lines of resonator

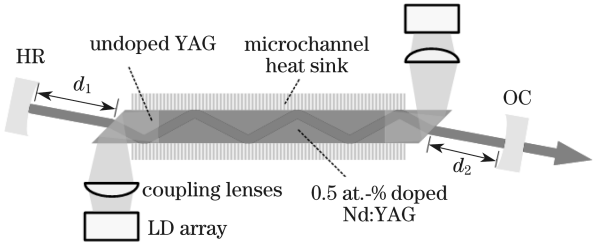

Fig. 1. Experimental setup of end-pumped zigzag slab laser.

mirror and of the slab end face. According to the diagram of geometry of the zigzag path in the slab shown in Fig. 2, the overall length of the slab can be described as

$$\begin{aligned} L_4 &= 2L_1 + 2L_2 + L_3 \\ &= Nt \text{ ctg } \gamma + t(\text{ctg } \alpha + \text{ctg } \gamma) \\ &= (N+1)t \text{ ctg } \gamma + t \text{ ctg } \alpha, \end{aligned} \tag{1}$$

where in this case $\alpha = 45°$ is the cutting angle at the slab end, $t = 2$ mm is the slab thickness, $L_4 = 78$ mm is the slab total length, N is an odd integral number representing times of TIR reflections, and

$$\gamma = 45° - \arcsin(\frac{n_{\text{air}} \sin\theta}{n_{\text{YAG}}}) = 45° - \arcsin(\frac{\sin\theta}{1.82}), \tag{2}$$

where n_{air} and n_{YAG} are the refractive indices of air and the slab, respectively. Thus the suitable incident angle θ for the laser beam to go through the slab and to be oscillated in the resonator can be calculated by combing Eqs. (1) and (2). The angle θ can be equal to 12.3° (when $N = 29$, $\gamma = 38.3°$), 15.8° (when $N = 27$, $\gamma = 36.4°$), 21.7° (when $N = 25$, $\gamma = 33.3°$), 23.6° (when $N = 23$, $\gamma = 32.3°$), and so on. It should be kept in mind that γ is supposed to be less than $90° - \theta_{\text{crit}}$ to ensure that the beam is confined in the slab through the zigzag path, where θ_{crit} is the critical angle at the TIR surface. As the TIR surface has a SiO_2 coating with the refractive index of 1.46, we obtain that $\gamma < 90° - \theta_{\text{crit}} = 90° - \arcsin(1.46/1.82) = 36.7°$. Therefore, the case of $\theta = 12.3°$ or of other incident angle with N larger than 29 is not available, and $\theta = 15.8°$ is chosen and expected to be the optimum incident angle because larger N results in higher mode matching factor between laser and pump modes, and thus higher output power.

In the experiment, we adjusted the location of the slab relative to the cavity mirror, and observed stable output with the aperture fully filled by the beam when the beam incident angle on the slab end is set at around 12°, 16°, 22°, and 24° individually as expected. Figure 3 depicts the output power from the oscillator as a function of the pump power at different incident angles, from which we can find that the case of incident angle of 16° gives the highest power, more than 20% higher than the other cases, and the output power decreaseds due to the reduction of N. The result has very good agreement with our calculation and discussion above. It should be noted that for a zigzag slab amplifier, in which the beam goes through the gain medium for once or a few times, there may not be a considerable change in the enhancement of output power with different N, but for a zigzag slab oscillator, the beam passes the slab for hundreds or thousands times, and the gain variation in a single pass with different N accumulates to be of a significant value.

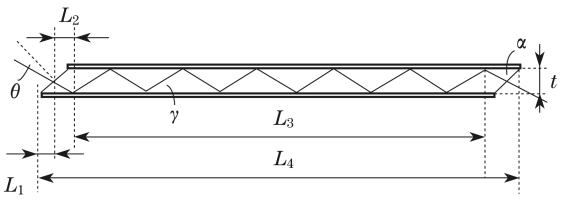

Fig. 2. Geometry of the zigzag path in the slab.

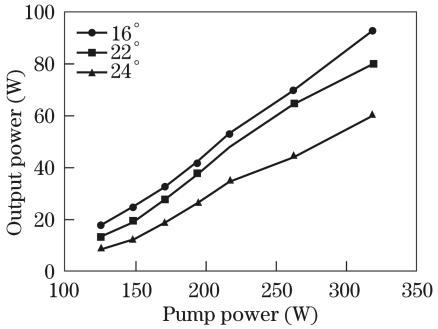

Fig. 3. Output power versus pump power for different incident angles on the slab end face.

The effective pump absorption coefficient for 0.5 at.-% Nd:YAG at 808 nm is $\kappa = 1.5$ cm^{-1}. When the crystal is pumped at 808 nm, in spite of the pump absorption efficiency of nearly 100%, the profile of the thermal loading that accounts for a fraction of 0.24 to the absorbed pump power in the slab is considerably non-uniform, leading to a large thermal gradient especially in the thermally bonding area, which has a negative effect in extracting output power from the resonator. In an attempt to reduce the thermal gradient, we set the LD array coolant temperature at 20°, and at this condition we measured, by the Agilent spectrum analyzer, the central wavelength of pump light emitting from the array as 803.2 nm. It can be estimated from the Nd:YAG absorption spectrum that the effective absorption coefficient for 0.5 at-% Nd:YAG at 803 nm is about $\kappa' = 0.7$ cm^{-1}, corresponding to a lower but acceptable absorption efficiency of 97% for the 50-mm-long doped gain medium we used. Figure 4 shows the absorbed pump density distribution along the length of the gain medium for both strong and weak absorption cases. As shown in Fig. 4, the pump density distribution becomes more uniform as the absorption is weakened. We tried different coolant temperatures of LD array, and found that the oscillator demonstrated the highest power at 20°C.

The output power extracted from the end-pumped zigzag slab resonator as a function of pump power is shown in Fig. 5. Pumping with a total power of 640 W of diode light yielded 253-W output power at 1064 nm, with a slope efficiency of 50.2% and an optical-optical conversion efficiency of 39.6%. The maximum average power of 290 W was achieved when the total pump power was 840 W, corresponding to an optical-optical efficiency of

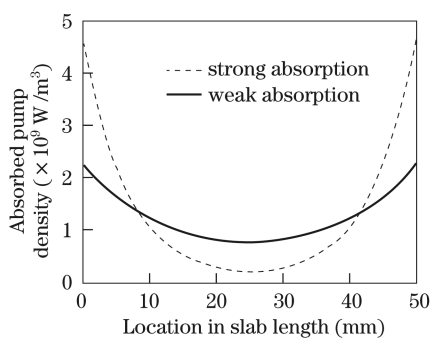

Fig. 4. Absorbed pump density distribution along the slab length for both strong absorption case ($\kappa = 1.5$ cm^{-1}) and weak absorption case ($\kappa' = 0.7$ cm^{-1}).

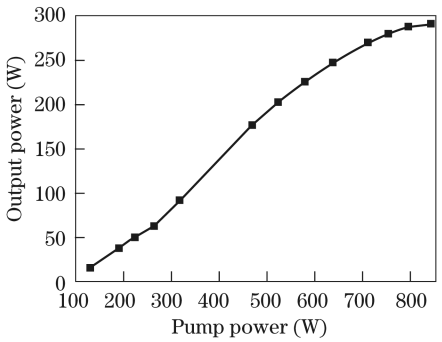

Fig. 5. Output power versus pump power for the oscillator.

34.5%. The instability of laser output at 250W was less than ±3%. The distinct decrease in the slope efficiency at high pump power is mainly due to the amplified spontaneous emission (ASE) effect. The laser output became clamped at the parasitic lasing threshold and very little additional output power could be obtained by increasing the pump power beyond 840 W. The beam quality of the laser output was estimated as about 3 and 10 in the slab thickness and width directions, respectively.

Different resonator structures have been adopted. Symmetric concave-concave cavity was proved to be the most stable and efficient structure in this case with the optimum output mirror with the transmission of 40%, while the output from the flat-flat cavity was clamped at the parasitic threshold with much lower pump power, and was quite unstable, varying significantly with a minor adjustment of the output coupler. Besides, the cavity with a cylindrical coupler focusing in the slab width direction produced higher laser output power than that with a cylindrical coupler focusing in the thickness direction, because the slab suffered more severe thermal lensing effect along the width than that along the thickness which had been compensated by the zigzag path.

In conclusion, with the prudent selection of incident angle, temperature tuning for the spectrum of the LD array, and resonator structure, we have demonstrated Nd:YAG zigzag slab oscillator with weak absorption that emits 253-W output power with a slope efficiency of 50.2% and an optical-optical conversion efficiency of 39.6%, and the maximum output power of 290 W is obtained with 840-W pumping power. In addition, we have confirmed that the performance of zigzag slab resonator depends sensitively on the incident angle of the beam at the slab end face.

This work was supported by the National Natural Science Foundation of China under Grant No. 50721004.

References

1. K. Tei, M. Kato, Y. Niwa, S. Harayama, Y. Maruyama, T. Matoba, and T. Arisawa, Opt. Lett. **23,** 514 (1998).
2. A. K. Sridharan, S. Saraf, S. Sinha, and R. L. Byer, Appl. Opt. **45,** 3340 (2006).
3. G. D. Goodno, S. Palese, J. Harkenrider, and H. Injeyan, Opt. Lett. **26,** 1672 (2001).
4. X. Cheng, Z. Wang, F. Chen, and J. Xu, Chin. Opt. Lett. **6,** 364 (2008).
5. X. Ma, J. Bi, X. Hou, and W. Chen, Chin. Opt. Lett. **6,** 366 (2008).
6. Z. Wang, J. Xu, and W. Chen, Chin. Opt. Lett. **5,** S36 (2007).
7. J. Li, X. Li, Y. Lu, and X. Zhu, Chinese J. Lasers (in Chinese) **33,** 289 (2006).
8. X. Li, J. Shao, H. Zang, and Y. Lu, Chinese J. Lasers (in Chinese) **35,** 206 (2008).
9. P. Shi, H. Zhang, Y. Wang, R. Diart, and K. Du, Acta Opt. Sin. (in Chinese) **24,** 641 (2004).
10. M. Guo, J. Li, W. Fu, X. Shi, Q. Hu, and W. Chen, Acta Opt. Sin. (in Chinese) **27,** 280 (2007).
11. G. D. Goodno, H. Komine, S. J. McNaught, S. B. Weiss, S. Redmond, W. Long, R. Simpson, E. C. Cheung, D. Howland, P. Epp, M. Weber, M. McClellan, J. Sollee, and H. Injeyan, Opt. Lett. **31,** 1247 (2006).
12. S. Palese, J. Harkenrider, W. Long, F. Chui, D. Hoffmaster, W. Burt, H. Injeyan, G. Conway, G. Truong, and F. Tapos, in *OSA Trends in Optics and Photonics, Vol. 50* C. Marshall, (ed.) (Optical Society of America, Washington, 2001) pp.41−46.
13. J. P. Machan, W. H. Long, Jr., J. Zamel, and L. Marabella, in *Technical Digest of 2002 Advanced Solid-State Lasers Conference* 549 (2002).
14. H. Kiriyama, K. Yamakawa, T. Nagai, N. Kageyama, H. Miyajima, H. Kan, H. Yoshida, and M. Nakatsuka, Opt. Lett. **28,** 1671 (2003).
15. H. Kiriyama, T. Yoshida, M. Yamanaka, Y. Izawa, T. Yamanaka, S. Nakai, T. Kanzaki, H. Miyajima, M. Miyamoto, and H. Kan, Fusion Eng. Design **44,** 419 (1999).